

The Effect of Dimensional Accuracy on Gear Tooth Contact Stress Due to the Casting Process

Joao B. Belo, Natalino Fonseca D. S. Guterres, Justiniano S. Guterres, Lidio I. Freitas, Lino Mendonca

Department of Mechanical Engineering, Dili Institute of Technology, Dili, Timor-Leste Dili Institute of Technology, Dili, Timor-Leste

Email: natalinofonseca81@gmail.com, [boscobelo74@gmail.com](mailto:boscobel074@gmail.com), salvadorguterres@gmail.com, lidiofreitas00@gmail.com, mendoncalino7@gmail.com

ABSTRACT

Gear dimensional accuracy is principally determined by whether the teeth slip when the gear rotates at high speed. However, it is necessary to pay attention to the dimensions of the tooth profile during the gear production process. The casting method is one of the methods used in gear production for forming a tooth profile, which is then followed by the machining process and surface hardening as a finishing step. The thing that needs to be considered is dimensional accuracy, which greatly affects the contact stress and decreases transmission power. The research aims to analyze the surface hardness and contact stress through FEM after dimensional change due to casting. The casting material is nodular cast iron, the mold is made of silica sand, and it is in closed molding condition. The gear pattern is made of four parts with different dimensions. The surface of the gear tooth is characterized by a chill, so that the casting will run simultaneously with the surface hardening. Surface area occurs at a high hardness of 720 HV. The average error value for all gears is 0.023 mm, and the contact stress and safety factor values after the static simulation are above the average value of 1. These results still meet the standards permitted by ISO and ANSI/AGMA standards.

Keywords: Spur gear, chilled casting, tooth stress, hardness, accuracy dimension.

Received January 16, 2023; Revised: March 20, 2022; Accepted May 02, 2023

1. Introduction

Gears are one of the components that transmit rotation and power as well. Because of the simple shape of the teeth, this type of spur gear is still widely used as a transmission component (Nisbett B., 2006). The application of spur gears in various industries, such as the automotive industry, manufacturing machinery industry, agricultural industry, and other industries. The agricultural industry is currently very much needed in Timor Leste, but the industrial equipment owned needs to have good performance. For example, the specific hand tractor equipment in the gearbox must be of good quality. In addition, there are also automotive industries such as motorcycle and car repair shops that have been opened in Timor Leste. The problem that is often handled by mechanics is gear transmission, but the main aspect is the quality of the gears, especially the materials used. Thus, it is necessary to involve scientists in academia to investigate the quality of components and analyze the work function of each component so that it can be overcome utilizing modifications developed through experimental research and new production plans. Observed from the function of the gears, when the gears operate and the cog teeth slip, the surface of the teeth often wears out and cracks. Surface hardness is one of the influencing factors; dimensional accuracy is not appropriate; and the material used (Davis, J.R., 2005). In addition, there are several standards such as ISO, DIN, and ANSI/AGMA that

determine the safety factor of the gear load capacity. This will be known through the analysis of the minimum value of power load (SH^2), which causes pitting as seen in the ISO 6336-2 (2006) standard, and for tooth bending fatigue as seen in the ISO 6336-3 (2006) standard. Some of the factors that influence it are the material properties, which are discussed in the ISO 6336-5 (2003) standard, loading limits, dimensional tolerances in the manufacturing process, and the lubrication system, which must match the function of the gears.

Gear machining and gear casting are the most common methods for producing gears, followed by surface hardening (Gupta K. and Kumar Neelesh K. J. 2017). For the gear casting process, the gear is cast using cast iron material so as to form the appropriate tooth profile, then machined and finished with surface hardening (Bralla, 1986). Many gears and other components are cast using nodular cast iron because nodular cast iron has advantages such as high ductility and easy formation of complex components compared to other cast irons (Olawale et al., 2016; Cardoso et al., 2014; Callister W. D. and Rethwisch D. G., 2010). Many methods have been used for gear surface hardening, including induction surface hardening (Barglik et al., 2018; Guterres, et al., 2017); flame hardening; plasma hardening (Cao et al., 2016); carburizing hardening (Wang et al., 2021); through hardening, and so on.

Based on the recommended requirements of the ANSI/AGMA 2001-D04, 2004 standard, the gears really need high hardness on the surface, but in the center zone, they remain ductile so as to prevent tooth stress and cracks in the tooth root area. The outer skin layer must be hard because it has high wear resistance. The required hardness value on the tooth profile surface is between 500 and 700 HV, depending on the function of each gear (Guterres, et al., 2017b; Čula et al., 2022; Guterres, et al., 2017a). For the application of gears in the transmission system, it is also necessary to pay attention to the value of dimensional accuracy in the tooth profile, especially on the tooth thickness, pitch circle diameter, and addendum circle diameter. While the gear teeth touch each other to transmit the load smoothly so as to prevent energy loss, it is necessary to have a good circle in the tooth profile and for the shape and dimensions of the tooth profile to be accurate (Radzevich S.P. 2012; Conrado et al., 2017; Bodzás, 2019). Dimensional accuracy values that are not in accordance with the gear function standard will provide slack between the driving gear and the pinion gear, resulting in fatigue contact and causing high noise (Yao et al., 2021); besides that, they will decrease power in the transmission system (Zhang et al., 2022). The most important area in the tooth profile is the tooth flank, so design errors, measurement process errors, and the equipment used to measure in the tooth flank area will have an impact on the precise dimensions that will cause noise and vibration, then increase the load-carrying capacity of gears in the transmission gearbox (Komori et al., 2009; Jolivet et al., 2013).

Based on the previous case study, our research team wanted to try to make gears using the casting method using nodular iron material. The surface hardening method used the chill, thus allowing one to analyze surface hardness and dimensional error on the tooth thickness area and observe the magnitude of the tooth stress when the gear shift slips. The hypothesis of this study is that the casting of gears using chill is intended to increase the hardness on the surface, but it is necessary to pay attention to the dimensional accuracy on the tooth profile because the casting process using the chilled casting method often results in shrinkage and expansion, which results in changes in the dimensions of the tooth profile, especially on the tooth thickness area. If there is a change in dimensions, the dimensional accuracy will deteriorate. Thus, the test was carried out to try to compare the dimensional error values to observe the magnitude of the tooth contact stress after the gear engages through simulation using Finite Element Methods (FEM). Using different dimensional patterns and molds will overcome the dimensional tolerance value at the time of casting. This method is very simple because the process of making gears is very short, thereby saving the cost of the gear production process. From the research highlights, it can provide new ideas to academics in the mechanical engineering department and to producers in production and manufacturing,

especially manufacturing of mechanical components, while also providing opportunities for researchers to follow up on related research.

2. Literature Theory

2.1. Basic Gear Fundamentals

Gears are components that are round and have teeth that are used to transmit rotary motion and transmit power from one shaft to another. Gears can generally be divided into several types, consisting of spur gears, miter gears, cone gears, worm gears, and others (Mott R. L, 2004). The spur gear indicates the direction of cutting the teeth on this type of gear in the direction of the axis. In addition to spur gears, there are also other types of straight teeth, namely those on the elongated rectangular rod. The direction of cutting the teeth can be perpendicular and can also form an angle with the tooth shaft (tooth body) (Mott R. L., 2004). The nomenclature of the spur gear can be seen in Figure 1, and the description can be explained as (a) module (m) is the length of the pitch circle diameter for each tooth. The unit for the module is a millimeter. (b) Circular pitch (p) is the distance measured on the pitch circle from one side of the tooth to the same side of the next tooth. (c) Clearance is the radial distance from the top end of one tooth to the bottom of the other for a gear pair. (d) The diameter of the flank is the distance whose length is equal to the diameter of the pitch circle plus two addendums. (e) Tooth thickness is the distance of tooth thickness measured on the pitch circle from one side to the other on the same tooth.

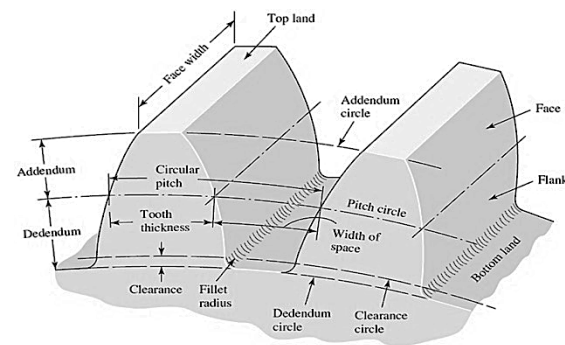


Figure 1. Spur gear nomenclature, (Nisbett B., 2006).

2.2. Standard size tolerances and spur gear series

Based on the AGMA 2000-A88 standard "Gear Classification and Inspection Handbook," the tolerance size for tooth thickness allowance due to impact loads for modules is from 1.0 to 3.0, which can be given in e25 DIN 3967, which has the highest tolerance value of 0.022mm and the lowest of 0.020mm. Meanwhile, spur gears with an outer diameter of 50 mm to 100 mm and modules from 1.6 to 3 can be assigned to e25 DIN 58405, where the highest contact

clearance value is 0.063 mm and the lowest is 0.022 mm (AGMA 341.02, 2004). The standard value for dimensional changes between the center point distance of the driving gear and other driven gears is 0.050mm; the change in tolerance at the highest center distance is 0.050mm, but this only applies to gears whose contact angle is 20. As for the contact effect caused by changes in tolerance, the standard maximum value is 0.036 mm.

JIS B 1701 standard module series (1973). The value of the module is based on the JIS B 1701 (1973) standard, which states that there are several levels of series, namely series 1, series 2, and series 3. In the series selection rules, prioritize the first series; if by compulsion, then you can choose the second and third series (Sularso and Suga, K. 2004; Lawson, 2004). Then came a new standard that was developed from the AGMA 2000-A88 standard to the ANSI/AGMA 2015-1-A01 standard, which included a gear tolerance standard that was scaled to 10 grades of A2-A1 accuracy values, besides that the precision was low, and then included the previous standards on quality class 13 with codes Q3-Q15, which include more precise tolerance qualities. The tolerance value for the tooth thickness area on the spur gear with module 8 and grade A is 0.302 mm. In addition, in the publication of the latest standards, they can be divided into three tolerance categories for accuracy, including high accuracy values (A2-A5), medium accuracy values (A6-A9), and low accuracy values (A10-A11) (Gupta K. and Jain N.K. 2017).

One of the factors that affects gear performance in the manufacturing process is the accuracy of the gear geometry. Gupta K. and Jain N.K. (2017) conducted functional inspection on several items that needed to be analyzed to obtain accurate and predictable dimensions through standard deviation values as seen in Figure 2 regarding the concept of pitch error and several profiles such as profile error, lead error, pitch error, run out error, and variations of tooth thickness.

2.3. Gear profile design

Gear teeth are a series of cam surfaces that contact similar surfaces on a mating gear in an orderly fashion. To drive in a given direction and to transmit power or motion smoothly and with a minimum loss of energy, the contacting cam surface on mating gears must have properties such as the gear height and the lengthwise shape of the active profiles of the teeth must be such that, before one pair of teeth goes out of contact during mesh, a second pair will have picked up its share of the load. This is called continuity of action. Another property is that the shape of the contacting surfaces of the teeth (active profiles) must be such that the angular velocity of the driving member of the pair is smoothly imparted to the driven member in the proper ratio. The most widely used

shape for active profiles of spur gears that meets these requirements is the involute curve.

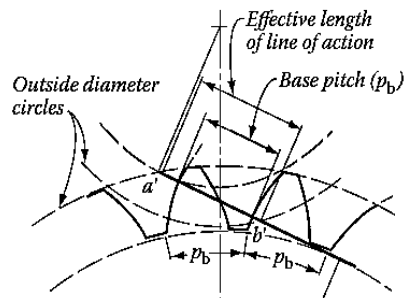


Figure 2. Gear teeth operation at the tooth action (Radzevich S.P., 2012).

Before the first leave mesh, the surfaces of two gears are in a good position to receive the load. Continuity of action and conjugate action are achieved by proper selection of the gear tooth proportions. Manufacturing tolerances on the gears govern the spacing accuracy of the teeth. Thus, to achieve a satisfactory design, it is necessary to specify correct tooth proportions, and, in addition, the tolerances on the tooth elements must be properly specified. All gear tooth contact must take place along the "line of action". The shape of this line of action is controlled by the shape of the active profile of the gear teeth, and the length of this line of action is controlled by the outside diameters of the gears. During part of the meshing cycle, two pairs of teeth will be sharing the load. The second pair of teeth must be designed such that they will pick up their share of the load and be prepared to assume the full load before the first pair of teeth goes out of action. Control of the continuity of action in internal-type spur gears is achieved by varying the operating pressure angle. The area of tooth action is shown in Figure 3. Gear teeth are a series of cam surfaces that act on similar surfaces of the mating gear to impart a driving motion. Many different shapes of surfaces can be used on the teeth to produce uniform transmission of motion. Curves that act on each other with a smooth driving action and a constant driving ratio are called conjugate curves (Radzevich S.P., 2012). And it can also be explained by the following studies: Kayabasi and Erzincanli (2007); Antoni A. et al. (2013) and Kolivand & Kahraman (2009).

2.4. Tooth thickness

The thickness of gear teeth determines the center distance at which they will operate, the backlash that they will have, and, as discussed in previous sections, their basic shape. The establishment of tooth thickness is one of the most important calculations made during the design of gear teeth. It is essential to specify the distance from the gear axis at which the desired tooth thickness is to exist. The usual convention is to use the distance that is established by the theoretical

pitch circle. Thus, if no other distance is shown, the specified tooth thickness is assumed to lie on the standard pitch circle. In certain cases, the designer may wish to specify a thickness, such as the chordal tooth thickness, at a diameter other than the standard pitch diameter. This specified diameter should be clearly defined on the gear drawings. The actual calculation of tooth thickness is usually accomplished by the three procedures described by Radzevich S.P. (2012). The teeth are finally given an allowance for machining tolerance. This tolerance gives the machine operator a size or processing tolerance. Usually, this is a unilateral tolerance. The gear teeth generated by a specific basic rack can have different tooth thicknesses, and the outside diameters of such gears are altered from standard as a function of the change in tooth thickness. In practice, these tooth profiles are achieved

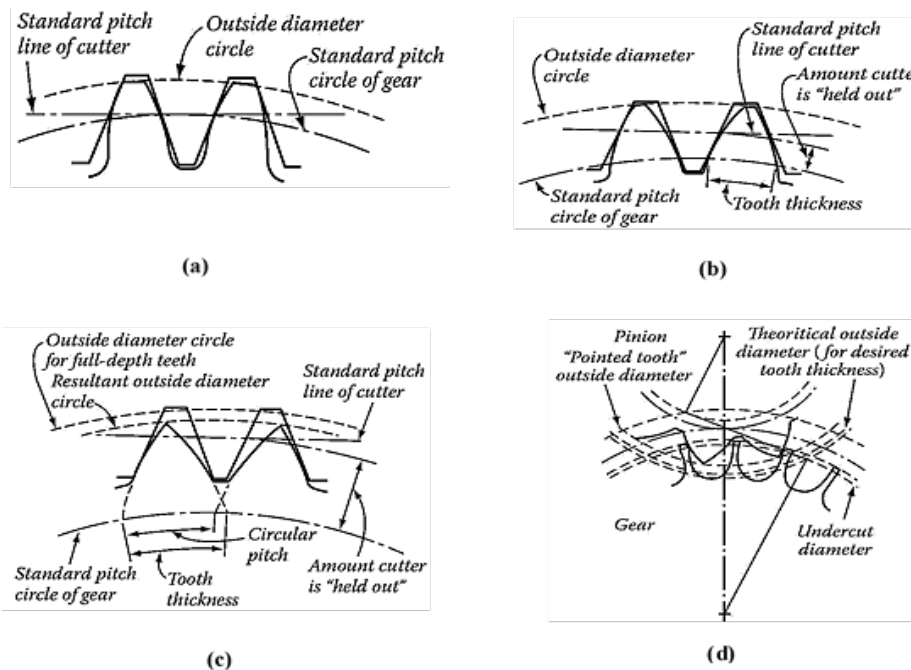


Figure 3. Tooth profile analysis (a) Cutting long-addendum teeth. (b) Standard tooth; (c) long-addendum (pointed) tooth; (d) long-addendum (over-enlarged) tooth (Radzevich S.P., 2012)

In Figure 3, four gears all having the same number of teeth, diametral pitch, and pressure angle are shown. In Figure 3a, the cutter shown by a rack has been fed to the standard depth. The outside diameter of this gear is standard, $(N+2) Pd$. Note the tooth thickness at the tip. In Figure 4b, the outside diameter was somewhat enlarged, and the cutter fed in the standard whole-depth distance starting from the enlarged outside diameter. This results in the thicker tooth (which would operate correctly with a standard gear on an enlarged center distance) and a somewhat thinner tip. Figure 3c shows what happens if the maximum outside diameter and tooth thickness are exceeded. The resulting tooth does not have the

by "feeding in" or "holding out" the gear-generating tools. It is customary to feed a specific cutter to a definite depth into the gear blank that has a larger than standard outside diameter. The cutter, when working at its full cutting depth, will still be held out from the standard N/Pd pitch circle (Razevich, S.P., 2012). Teeth generated thicker than standard will have tips of a smaller width than standard since the cutter must be "held out." For any given number of teeth, the tooth thickness can be increased such that the tip will become pointed at the outside diameter circle (Razevich S.P., 2012).

a point of maximum compressive stress. Directly underneath this point, there is a maximum subsurface shear stress. The depth to the maximum shear stress is slightly more than one-third the contact band width (Radzevich S.P., 2012).

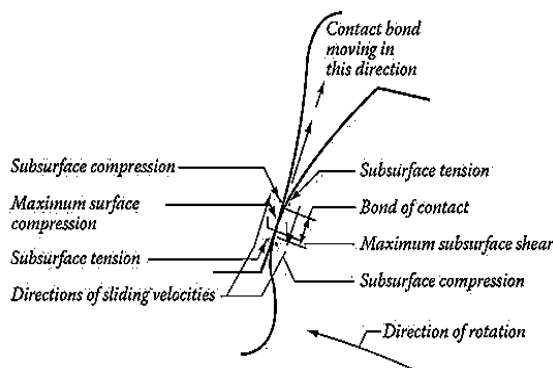


Figure 4. Stress in region of tooth contact (Radzevich S.P., 2012)

The gear tooth surfaces move across each other with a combination of rolling and sliding motions. The sliding motion and the coefficient of friction tend to cause additional surface stresses. Just behind the band of contact, there is a narrow region of tensile stress. A bit of metal on the surface of a gear tooth goes through a cycle of compression and tension each time a mating gear tooth passes over it. If the tooth is loaded heavily enough, there will usually be evidence of both surface cracks and plastic flow on the contacting surface. There may also be a rupturing of the metal as a result of subsurface shear stresses (Radzevich S.P., 2012).

2.6. Chill and Denseners

Chill is a high thermal conductivity material or component used to accelerate metal cooling in the mold. Hurst S. (1996) describes a chill made of copper or cast iron that is placed on the surface of the mold to regulate rapid cooling on the surface of the specimen to be cast. A chilled solid is introduced into the mold at the surface of the specimen or protrudes into the mold cavity to cause solidification in the mold. The molten metal surrounds the chilled density during casting. If chill is made from a material, it will be combined (Campbell, J., 2011). Many studies have been conducted to investigate the use of chill for structural recrystallization on the surface of cast steel specimens (Jaromin et al., 2019; Dommarco & Salvande, 2003; Kanthavel, 2014). Chill copper casting explained by (Mehr et al., 2014); and chill aluminum casting explained by (Pavithra and Prasad A., 2018; Wankhede et al., 2018; Wankhede et al., 2017). Chilling has also been used to harden the surface of nodular cast iron (Qian et al., 1996).

In general, there are different grain structure regions in metal casting (Piwonka, 1998). Very small crystal cold regions are produced by fast cooling rates at very extreme edges; the long and very thin columnar crystal region lies along the direction of the heat flow and extends inward from the cold region; and crystal regions with coarse size variations are approximately at the center or center of the casting. The grain boundaries represent the meeting point of the various nuclear growths that were originally formed. When cooling is rapid, more grains will develop and grow to fill nearby cavities. If more grains are formed and the grain size in the metal solidifies more finely, then that is what is called the grain crystal structure. It seems that white cast iron is very hard on the surface of the casted specimen, which can be seen more clearly in Figure 6a (Hurst S., 1996).

The final grain size depends, to a large extent, on the cooling rate. When the cooling rate cannot be controlled, the desired fine grain size can be promoted by introducing foreign nuclei into the metal to cause crystal growth to start in more places (Hurst S., 1996; Campbell J., 2011). Another method is to form a chill on the mold wall on the inside of the mold so that the liquid poured into the mold quickly transforms into cooling until there is rapid solidification on the outer layer of the specimen so that a rapid growth of dendritic structure is formed in the skin layer, as shown in Figure 6b, which is easy to happen because contact between the chill-coated mold cylinder wall and the solid specimen occurs (Beddoes J. and Bibby M. J., 2003).

3. Research Metodology

In this study, the methods used for the processes of data collection and data analysis are a quantitative method and a descriptive method. These two methods are: the number of certain test points on the gear sample will be representative of other test points, and the discussion of the data results will take the average value to be inputted in the simulation process so as to know the static stress on the gear tooth profile. The stages of the research include Politeknik Manufaktur Ceper Klaten, PT ATMI IGI Center Surakarta, Material Test Laboratory UGM Yogyakarta, and Laboratory of Training Center UNDIP Semarang after determining the location of the casting and the location of the sample testing. The next step is to start with the selection of materials for testing, the casting and surface hardening processes, the gear tooth profile cutting process, inspection, and testing. The final step is the simulation process to determine tooth stress based on the gear manufacturing system (Gupta K. and Jain N. K., 2017). The next step is analysis and discussion; the last step is drawing conclusions and making recommendations.

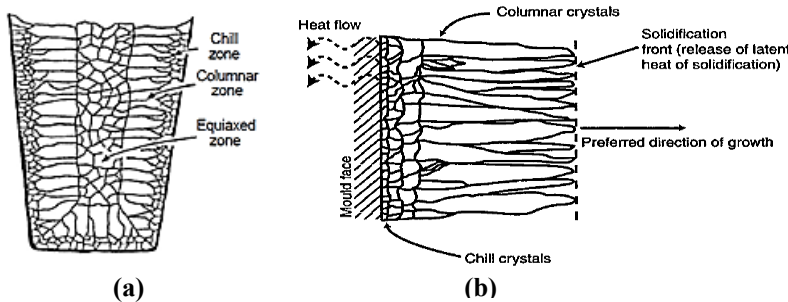


Figure 6. Chill function (a) Imagination of macrostructure and grain structure (Hurst S., 1996) (b) Crystal structure solidification process in the mold (Beddoes J. and Bibby M. J., 2003).

3.1. Data Collection

The types of data that need to be collected in this study consist of gear dimensions, hardness values, and dynamic stress values of the gears. But the first step is the selection of material for gear casting.

The material for casting gears is scrap steel and scrap iron, which must be cut sufficiently to be put into a crucible with

a capacity of 25 kg, then melted at a maximum temperature of 1500 °C and a pouring temperature of 1200 °C, as implemented by Escobar et al. (2015). To obtain pearlitic nodular cast iron specifications, 5% Fe-Si-Mg alloy for spheroidization was used followed by post-inoculation with 75% Fe-Si, the same method as research conducted by Abedi et al. (2010) and Jafar and Behnam (2011). The chemical composition of the produced nodular cast iron is presented in Table 1.

Table 1. The chemical composition (wt. %) of nodular cast iron.

Alloy	C	Si	Mo	Mn	Mg	Ni	Cu	P	S	Cr	Fe
(wt.%)	3.58	2.50	0.007	0.22	0.02	0.121	0.04	0.012	0.004	0.04	Balance

The material for use in the chill is austenitic stainless-steel SUS 316L, which functions as a high cooling rate on the surface of the cast specimen so that it can harden the surface of the gear tooth profile, as has been applied in previous studies by Qian et al. (1996). The chemical composition of SUS 316L chill material can be listed in Table 2, where, according to the ASM Handbook (Washko S. D. and Aggen G., 1990),

shown in Figures 7b, 7c, and 7d, will be fitted into the sand mold. However, the GA gear pattern (Fig. 7a) functions as a reference pattern, and the reference pattern functions to create GB, GC, and GD patterns to produce different dimensions. The reference pattern also functions as comparative dimensional data.

Table 2. The chemical composition (wt. %) of SUS 316L.

Alloy	C	Mn	Si	Cr	Ni	P	S	Mo
(wt.%)	0.03	2.00	1.00	17.03	11.43	0.041	0.04	2.00

3.2. Gear casting process

At this stage, patterns, chill and sand molds have been prepared according to plan so that the casting process can run smoothly. The chill used is in the form of a plate with a thickness of 1 mm to be folded into three selected teeth consisting of gear number 3, tooth number 5, and tooth number 10 as shown in Figure 7. Three gear patterns, such as gears GB (gear B), GC (gear C), and GD (gear D), as

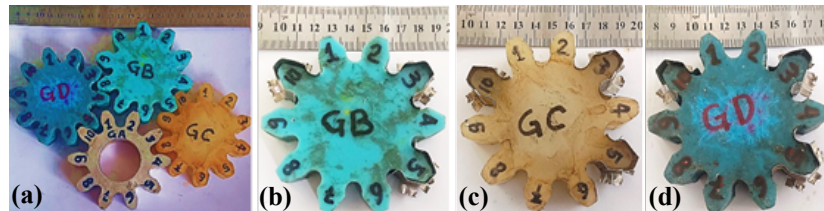


Figure 7. Chill and gear pattern (a) The resin gear pattern and benchmark gear (GA) (b) three teeth of GB sample gear selected for chill installation (c) three teeth of GC sample gear selected for chill installation (d) three teeth of GD sample gear selected for chill installation.

Making sand molds and their composition was done as has been done in previous studies by Guterres, N.F.D.S. et al. (2021a). A Silica sand mold is a closed form, as shown in

Figure 8b. Furthermore, the pouring step is carried out in three molds that have been prepared simultaneously (Fig. 8b).

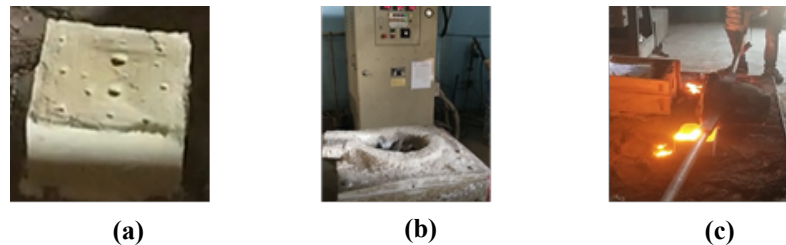


Figure 8. Gear casting process (a) closed silica sand mold (b) raw material filling and smelting process (c) pouring step.

3.3. Data Analysis

In this study, the type of data that needs to be collected consists of dimensional measurement data to determine the dimensional changes on the gear tooth profile, Vickers hardness data to determine the hardness value of the outer skin layer on the gear tooth profile, and tooth static simulation to determine the stress analysis value obtained from the dimensional inspection, hardness testing, and finite element analysis, respectively.

3.1.1. Dimensional measurement and data analysis

Dimensional measurement data (gear inspection) is taken in 3 stages. The first stage is measuring the gear pattern, the second stage is measuring the dimensions after the gear is cast, and the third stage is measuring the gear due to EDM-wire cutting. The inspection for the second stage is after the gear is cast to determine the thickness of the cut in the tooth profile using EDM-wire cutting as has been used in previous studies by Gupta and Jain (2014); Gupta and Jain (2013); Alhadeff et al. (2018); Chaubey and Gupta (2022).

To measure the tooth thickness by using the Profile Projector, the Starrett VB400 is equipped with a Quadra-Chek 200, which functions to record measurement results as shown in Figure 9a. The principle of measurement has been described in previous research by Pillarz M. (2020), Guterres et al. (2017b), and Keyence (2022).

The most important area in the tooth profile that needs to be measured is the tooth thickness, as shown in Figure 9b,

because if dimensional distortion occurs in the tooth thickness, it will affect the accuracy in the tooth flank (Stöbener et al., 2012). This tooth thickness area was measured for all teeth in each gear sample. Each tooth was measured three times, and the results were averaged for analysis and discussion.

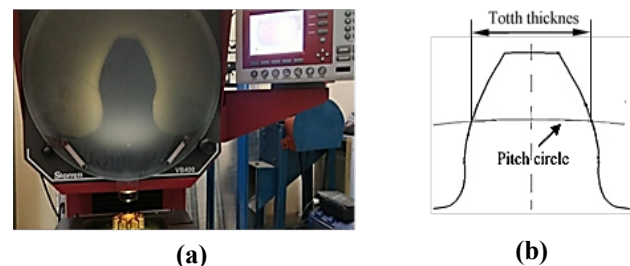


Figure 9. Measurement area on the tooth profile.

To measure the tooth thickness by using the Profile Projector, the Starrett VB400 is equipped with a Quadra-Chek 200, which functions to record measurement results as shown in Figure 9a. The principle of measurement has been described in previous research by Pillarz M. (2020), Guterres et al. (2017b), and Keyence (2022).

The most important area in the tooth profile that needs to be measured is the tooth thickness, as shown in Figure 9b, because if dimensional distortion occurs in the tooth

thickness, it will affect the accuracy in the tooth flank (Stöbener et al., 2012). This tooth thickness area was measured for all teeth in each gear sample. Each tooth was measured three times, and the results were averaged for analysis and discussion.

All the data taken from the measurement results will be processed with Microsoft Excel and then analyzed. From the results of the value in the table, we can see a change in the dimensions of the tooth thickness based on the observation of different dimensions. The difference between this value and the error number is called the dimensional tolerance between the gears when they slip into each other.

Table 3. Mechanical Properties of the Gear Material.

Material Grade	Hardness (HV)	Tensile Strength (Mpa)	Yield Strength (Mpa)	Poisson's Ratio	Density (g/cm ³)	Modulus Young (GPa)	Elongation (%)
Pearlitic Ductile Iron	200	689	483	0.31	7.84	168	3

3.1.3. Hardness testing and data analysis

To determine the microhardness on the tooth profile area by using a Vickers Buehler MMT-7 microhardness tester under a load of 200 g, like the method that has been carried out in related research by Sohi et al. (2012). The hardness testing process is carried out on the tooth profile after the profile cutting process.

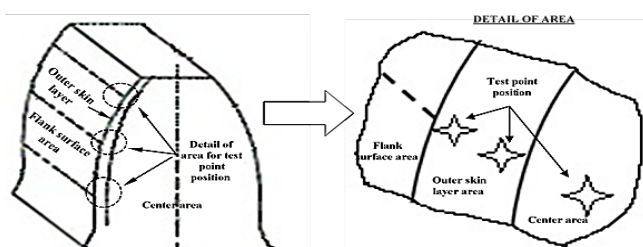


Figure 10. The position of the Vickers test point in the tooth profile area.

This test method uses the destructive method, meaning that the gear will be cut by 3 teeth to represent the average hardness value in the tooth profile. Microhardness tester samples were sectioned into the proper size and polished with 80, 150, 1200, and 2000 grinding papers, respectively. The test point on the tooth profile is in the outer skin layer area toward the center of the gear (Jamari et al., 2021), as

3.1.2. Gear simulation process

The gears will be 3D modeled using Finite Element Analysis (FEA) software with different tooth thickness dimensions, and simulations will be run to determine the contact stress and safety factor value. FEA can be used to determine gear tooth conditions such as tooth stress when given dynamic loads based on safety factor values, as has been done in related studies by Kumar et al. (2021), Kumar et al. (2022), Barka (2017), Schneider et al. (2022). The data from the gears needed for the simulation can be found in Table 3. Based on the ASTM A 536 standard (Lyle R. J. 2005), the material type is pearlitic ductile iron.

shown in Figure 10. The number of test points on the tooth surface is six, and the distance from one test point to another is 0.2mm, 0.4mm, 0.8mm, 1.2mm, 1.6mm, and 3mm, respectively.

Hardness value data will be displayed in a table and analyzed through graphs to compare the surface and the center zone.

4. Results

The sequence of data displayed in this result and discussion was originally the result of dimensional measurements. The dimensional data that will be discussed is the error value after the tooth sample is measured on the tooth profile, especially on the tooth thickness. The next data that needs to be displayed is data from simulation results, such as tooth stress analysis on the tooth profile. After that, the data from the Vickers hardness test showed results in the outer skin layer area.

4.1. Gear dimensional analysis

After measurements were made in the tooth thickness area for all GB, GC, and GD gear samples, the measurement data can be listed in Table 5. After the gears were cast, shrinkage defects and expansion defects occurred in most of the teeth and then the gears followed by the EDM-Wire Cutting process as used by (García-H et al., 2016) to get the final dimensions. Furthermore, to find the error value in the tooth thickness area, the dimension value of the GA (gear benchmark) gear will be reduced by the dimension value after the profile cutting.

Table 4. Dimensional Measurement Result of the GBGear Sampel.

Tooth number	T1	T2	T3	T4	T5	T6	T7	T8	T9	T10
GA (gear benchmark)	16.010	15.417	15.793	16.170	15.947	15.993	16.053	15.533	15.347	16.040
GB (After Casting)	15.912	15.707	15.689	16.192	16.157	15.911	16.051	15.389	15.233	16.282
GB (After profile cutting)	15.961	15.562	15.741	16.181	16.052	15.952	16.052	15.461	15.290	16.161
The error value	0.049	-0.145	0.052	-0.011	-0.105	0.041	0.001	0.072	0.057	-0.121

Table 5. Dimensional Measurement Result of the GC Gear Sampel.

Tooth number	T1	T2	T3	T4	T5	T6	T7	T8	T9	T10
GA (gear benchmark)	16.010	15.417	15.793	16.170	15.947	15.993	16.053	15.533	15.347	16.040
GB (After Casting)	17.021	16.114	16.584	17.113	17.028	17.113	17.084	16.462	16.141	17.012
GB (After profile cutting)	16.091	15.184	15.654	16.183	16.098	16.183	16.154	15.532	15.211	16.082
The error value	-0.081	0.233	0.139	-0.013	-0.151	-0.190	-0.101	0.001	0.136	-0.042

Table 6. Dimensional Measurement Result of the GD Gear Sampel.

Tooth number	T1	T2	T3	T4	T5	T6	T7	T8	T9	T10
GA (gear benchmark)	16.010	15.417	15.793	16.170	15.947	15.993	16.053	15.533	15.347	16.040
GB (After Casting)	17.121	17.001	17.191	17.471	17.129	17.134	17.183	17.000	17.011	17.200
GB (After profile cutting)	15.721	15.601	15.791	16.071	15.729	15.734	15.783	15.600	15.610	15.800
The error value	0.289	-0.184	0.002	0.099	0.218	0.259	0.270	-0.067	-0.264	0.240

This error value will be used as tooth thickness data when input into the 3D modeling process using Solidworks. As discussed in the research method, the teeth selected to determine the contact stress results consist of tooth number 1 (T1), tooth number 5 (T5), and tooth number 10 (T10). Then the results of the contact stress analysis can be compared between the GB, GC, and GD gear samples.

4.2. Gear tooth stress analysis

Straight gear samples were assembled using a 3D model created in SolidWorks for stress analysis. The gear sample parameters, gear material specifications, and gear specifications are as shown in Table 7 and input for the meshing process so that stress, displacement, strain, and safety factor values can be found by applying a static load of 3.56 N.m. and 1500 rpm repeatedly. At the beginning, the gear analysis step is modeled based on the dimensions of the casting result and followed by the finishing process (profile cutting), which can be illustrated through the image display as shown in Figure 11, and the dimensions in the tooth thickness area for all teeth will adjust the results after cutting the tooth profile as stated in Tables 4, 5, and 6. Gear nomenclature and tooth profile contact focal point parameters are important things that must be determined so that they can be used as input data for simulations. Besides that, the tooth area affected by contact stress can be

understood on the target. The next stage is the static simulation process to find the values of stress, displacement, strain, and safety factor. Other stages and simulation parameters that need to be adjusted consist of connections, fixtures, external loads, and mesh. At the connection stage, a contact is made between the two faces of the teeth, as shown in Figure 12a. The selected contact face is adjusted to the area of contact that the mate has made in the assembly process shown in Figure 11.

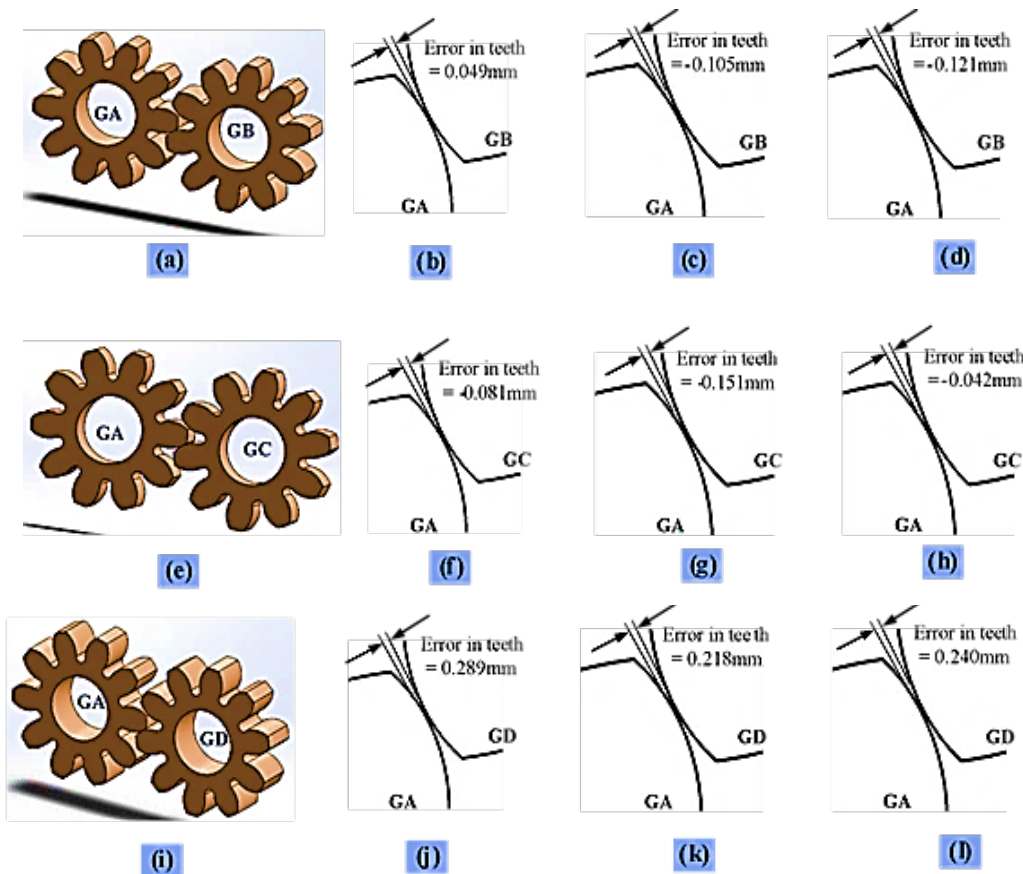


Figure 11. Gear modeling according to dimensions after profile cutting. (a) Gear sample GA and GB assembly (b) error value of GB and T1 (c) error value of GB and T5 (d) error value of GB and T10 (e) Gear sample GA and GC assembly (f) error value of GC and T1 (g) error value of GC and T5 (h) error value of GC and T10 (i) Gear sample GA and GD assembly (j) error value of GD and T1 (k) error value of GD and T5 (l) error values of GD and T10.

Table 7. Nomenclature and the Calculate Parameter of the Gear Pair

Gear Sample	Tooth Number	Tooth Thickness (mm)	The Error Value (mm)	Number of Teeth (Z)/(N)	Module (m)	Pressure angle (°)	Face Width (mm)
GA (benchmark)	T1	16.010	-	10	8	20	25
	T5	15.947	-				
	T10	16.040	-				
GB	T1	15.961	0.049				
	T5	16.052	-0.105				
	T10	16.161	-0.121				
GC	T1	16.091	-0.081				
	T5	16.098	-0.151				
	T10	16.082	-0.042				
GD	T1	15.721	0.289				
	T5	15.729	0.218				
	T10	15.800	0.240				

The next stage is the gear fixture process. In the process of this fixture, it will regulate the gears that are fixed and the gears that become fixed hinges, such as the gears from the casting results shown in Figure 12c. The first gear is the GA sample gear, which works as a fixed hinge as a gear that will

be connected to the shaft as a source of torque, while the second gear, namely the GB, GC, and GD sample gears, is fixed and will only rotate when it receives rotation from the GA sample gear, as shown in Figure 12b.

The external load process is to apply a torque force originating from the shaft that receives power from the motor as illustrated in Figure 12d. This analysis uses $\frac{3}{4}$ horsepower (HP) motor power and simulates acceleration gears from a

rotation speed of 1500 rpm, but the distribution of torque on the shaft and gear of the GA sample is 3.56 N.m. like the method applied by previous research, Fu et al., (2020).

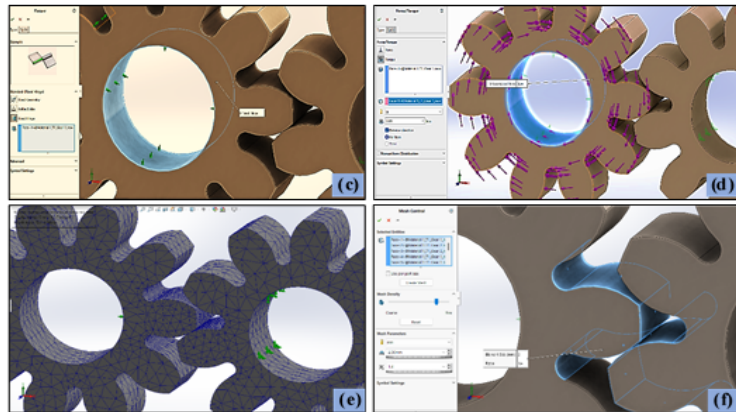


Figure 12. Gear simulation stage (a) setting the contact (b) setting up the casting gear for the fixed (c) setting up the sample gear GA (d) external load process to apply torque and power (e) Global mesh to control tooth contact area (f) local mesh all mesh area of gears.

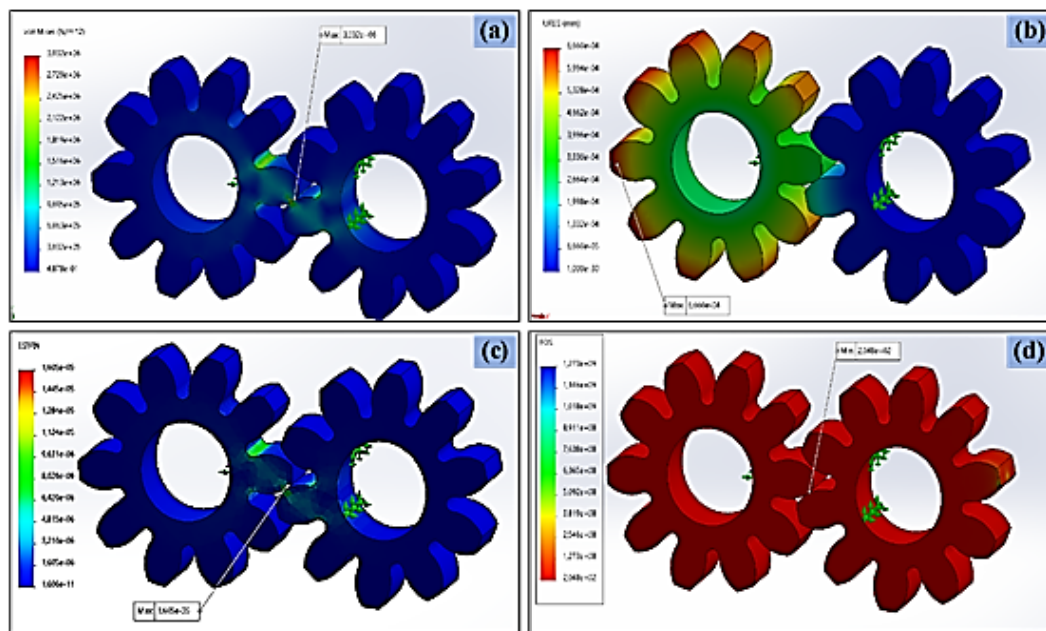


Figure 12. Static simulation results (a) Stress; (b) Displacement; (c) Strain; (d) Safety Factor.

Proceed with the gear meshing stages locally and globally. The global mesh was made in the tooth contact area with a size of 2 mm, as shown in Figure 12e, and the local mesh was made with a size of 5 mm in the control mesh section. Figure 12f. After finishing setting all the simulation parameters, the running process is continued to get the values of stress, displacement, strain, and safety factor. The contact

stress value will be obtained from the pressure between the surfaces of one tooth and another, so what you need to know is the allowable stress limit value. The action of the stresses on the two gears and the analysis of the stress values can be seen in Figure 12a. Displacement analysis can be used to analyze changes in tooth shape after receiving a force, as shown in Figure 12b. The allowable strain limits can be simulated as shown in Figure 12c, and in the end, the

minimum and maximum allowable limits can be taken from the safety factor simulation results as shown in Figure 12d. The results of all the simulated parameters will be displayed

in table form and can be seen in Table 8. Then all the data will be copied and compared to the gear that has the maximum error value and the minimum error value.

Table 8. Static Simulation Analysis of Gear Sampel After Finishing Product.

Simulation Parameters	Gear sampel GB			Gear sampel GC			Gear sampel GD		
	T1	T5	T10	T1	T5	T10	T1	T5	T10
Stress (N/mm ²)	5.726	3.202	3.058	3.045	3.215	3.036	3.142	2.911	3.065
Safety Factor	118.4	150.8	158.0	158.6	150.3	159.1	153.7	165.9	157.6

Table 8 displays the static simulation results with several simulation parameters to determine the gear contact stress of each tooth that was surface hardened using chill. In addition to surface hardening, another factor that needs to be investigated in this static simulation is the effect of the difference in dimensional error in the tooth thickness on the allowable tooth contact stress of all gear samples.

Contact stress analysis is important because contact stress failure also depends on manufacturing accuracy. ISO 6336-2 (2006) prohibits accuracy values from influencing gear quality. The contact stress value obtained from the simulation results is above the average value of 1, can meet the criteria of ANSI/AGMA standards 2001-D04 and 2101-D04 and are described by Nisbett, B., (2006) and the average value for all teeth after adding up is 3.378N/mm². The results of this contact stress value are obtained so that all gears after casting that have an average error value of 0.023 mm can still be used for operation at high rotation. Such results were investigated in related studies by Korta and Mundo (2011). In addition, the error value still meets the requirements based on the AGMA standard (AGMA 341.02, 2002). With an average error value of 0.023 mm obtained from dimensional changes in the tooth thickness area for all teeth, it meets the requirements of the ANSI/AGMA 2000-A88 standard, having a tolerance value of 0.302 mm. When applying these results to the static simulation process, it turns out that the gear operation is safe to use.

The analysis of the safety factor limit value is important because it is based on the recommendation from the safety factor function, which is to determine the factors in the process of making gears such as design analysis, material characteristics, and manufacturing tolerances (ANSI/AGMA 2101-C95, 2001). It is observed that the safety factor value of all simulation items applied to the tooth profile is above the value of 1 (one). These results still meet the standards permitted by ISO 6336-1 (2007). So it can be said that all tooth profiles that experience dimensional changes in the tooth thickness area using chill casting to harden the surface are declared safe when receiving contact loads from each contact point area at high rotation rates, as explained by a related study from Fu et al. (2020). Although the deformation values and strain values are not shown in table 8, the results were found after static simulation. The average deformation

value for all samples and all teeth was 0.000451 mm/s. while the average value of the strain received by the teeth of all gear samples is 0.0000128 mm/s.

Based on the value of the simulation results obtained, the value is below 1, thus the gear contact is still safe for operation at high rotation. Because the simulation results show that the stress value and the safety factor value are safe at the specified loading and at high speed, the results obtained from the gear accuracy inspection process are acceptable and still suitable for use.

4.3. Gear tooth hardenss analysis

As explained in the hardness testing method, the value of the Vickers hardness (HV) test results can be taken from the tooth profile, which is focused on the outer skin layer area toward the center area.

The results of the hardness test values are displayed in graphical form and will be analyzed for the effect of using SUS 316 stainless steel material on the hardness value and hardness layer thickness. For each gear sample (GB, GC, and GD), the average Vickers hardness value will be taken from the total teeth tested, such as T1, T5, and T10.

Therefore, the number of graphic lines to be displayed is 3, and the number of test points from the outer skin layer toward the center is 6 points. The test results and parameters can be found in Figure 13. It can be seen from the graphic line shown in Figure 13 that the surface area of the gear profile is harder than the middle area. The average hardness value on the entire surface of the gear is up to 708 HV. This value meets the gear hardness standard to be allowed to operate in the gearbox (ISO 6336-2, 2006).

The highest hardness value of the three gear samples was 730 HV, which occurred in the GC gear sample wheels with a hardness layer thickness of 0.2mm. The high hardness value is due to the presence of chill, and the function of chill is to cool the surface of the tooth profile so that the area touched by the chill is chilled earlier during the freezing step of the nodular cast iron material. With this faster cooling rate, it is predicted that the structural matrix formed on the chilled surface is the cementite phase; this is based on previous studies using the same type of chill material: Guterres et al., (2021a), Qian et al., (1996), and Guterres, et al., (2021b).

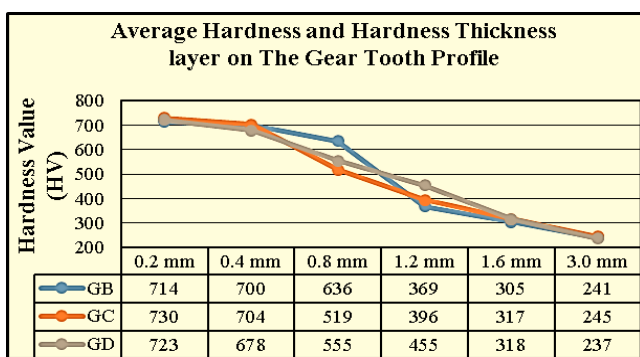


Figure 13. Average hardness value on the gear tooth profile after the gear profile cutting process.

Based on the results, dimensional error values, contact stress values, and hardness values were found and validated with AGMA standard guidelines, ISO, and relevant research. The spur gear casting process using chill for surface hardening does not cause significant dimensional changes to affect gear dimension accuracy. Therefore, in theory, the method used in this research, namely, gear chilled casting, is feasible to use because the gear manufacturing method can shorten the process and save costs. The practical implication is that designers, researchers, and the gear manufacturing industry can use this casting method to make gears in a short time and save on production process costs.

5. Conclusion

The hardness value, error value after the gear finishing process, and contact stress on the gear profile are all investigated in this study. After the results are obtained, this research can be concluded as follows:

1. After the gears are cast and proceed to the finishing process, the average error value found in the tooth profile for all sample gears is 0.023 mm. This value is still declared safe in the gear tooth profile design system based on ANSI/AGMA standards regarding gear accuracy tolerances.
2. After conducting FEM analysis using static simulation, the contact stress value and safety factor value of the teeth for all gear samples still meet the requirements based on ISO standards, which recommend the calculation of the load capacity of spur gear, and the AGMA standard regarding spur gear tolerance and measurements.
3. Using chill has resulted in a high cooling rate on the surface of the gear tooth profile, so that the average hardness value on the surface coated with chill with a distance of 0.2 mm–0.4 mm reaches 708 HV.
4. Based on the experimental and simulation results, it was found that using ANSI/AGMA standards to validate the dimensional accuracy test results is very necessary in gear

inspection. For academics, especially practice laboratories in the fields of production and manufacturing, to remain consistent in using the applicable standards for the validation process.

6. Recommendation and Future Research

1. Researchers are advised to try an analysis of changes in dimensions for the production of gears with small modules.
2. Based on the results found in this study, further research is needed to apply the chilled casting method to engine components that require high surface hardness for high wear resistance, such as camshafts, crankshafts, and cylinder blocks.
3. A more detailed analysis of the gear pattern dimensions is required before assembling the chill plate on the gear pattern profile to continue installation into the sand mold.

Acknowledgements

This work is financially supported by the Centre for Applied Research Policy Studies and Community Service (CARPS-CS) DIT, Timor Leste (Grant Number: 0009/CARPS-CS/DIT/VII/2022). The gear casting process was carried out at the Polytechnic Manufacture in Ceper-Klaten, Indonesia. PT ATMI IGI Center Surakarta and the Laboratory of Training Center Diponegoro University Semarang, both in Indonesia, provide assistance with gear testing and inspection.

References

Abedi H. R., Fareghi A., Saghafian H., and Kheirandish S. H., (2010) “Sliding wear behavior of a ferritic-pearlitic ductile cast iron with different nodule count,” Wear, vol. 268, no. 3–4, pp. 622–628.

AGMA 341.02, (1970) “Design of General Industrial Coarse Pitch Cylindrical Wormgearing” Design Manual for AGMA STANDARD, ANSI/AGMA., vol. 6022493. United State of America: AGMA Standard, p. 9.

Alhadeff L. L., Curtis D. T., Marshall M. B., and Slatter T., (2018) “The application of wire electrical discharge machining (WEDM) in the prototyping of miniature brass gears,” Procedia CIRP, vol. 77, no. Hpc, pp. 642–645.

ANSI/AGMA 2000-A88, (1988) “Gera classification and inspection Handbook: Tolerance and measuremnet methodes for unassembled spur and helical gears,” in Handbook, Partial Re., vol. 1988, no. AGMA Association, United State of America: American National Standard, p. 92-203.

ANSI/AGMA 2001-D04, (2004) "Fundamental Rating Factors and Calculation Methods for Involute Spur and Helical Gear Teeth," vol. 04, p. 66.

ANSI/AGMA 2101-C95, (2001) "Fundamental Rating Factor and Calculation Methods for Involute Spur and Helical Gear Teeth", Metric Edi. 2001, Alexandria, Virginia 22314: AGMA National Standard.

Artoni A., Guiggiani M., Kahraman A. and Haryanto J., (2013) "Robust Optimization of Cylindrical Gear Tooth Surface Modifications With Ranges of Torque And Misalignments," in Proceedings of the ASME 2013 International Design Engineering Technical Conferences and Computers and Information in Engineering Conference, vol. 77583, pp. 1–10.

Barglik J. et al., (2018) "Comparison of single and consecutive dual frequency induction surface hardening of gear wheels," IOP Conf. Ser. Mater. Sci. Eng., vol. 355, no. 1.

Barka N., (2017) "Study of the machine parameters effects on the case depths of 4340 spur gear heated by induction—2D model," Int. J. Adv. Manuf. Technol., vol. 93, no. 1–4, pp. 1173–1181.

Bodzás S., (2019) "Analysis of the effect of the addendum modification coefficient for contact surfaces of spur gear," Stroj. Cas., vol. 69, no. 1, pp. 5–16.

Callister W. D. and Rethwisch D. G., (2010) Materials Science and Engineering An Introduction, Eighth Edi. United States of America: Jhon Wiley and Sons, Inc, p. 402.

Bralla, J. G. (1986). Design For Manufacturability Handbook, Second Edi. McGraw-Hill, New York, NY 10011. United States of America, p. 689-704. www.digitalengineeringlibrary.com.

Cambell J., (2011) "Complete Casting Handbook Metal casting process, techniques and design", First Edit. United State of America: Elsevier Ltd, p. 185-219.

Cao H. T., Dong X. P., Pan Z., Wu X. W., Huang Q. W. and Pei Y. T., (2016) "Surface alloying of high-vanadium high-speed steel on ductile iron using plasma transferred arc technique: Microstructure and wear properties," Mater. Des., vol. 100, pp. 223–234.

Cardoso P. H. S., Israel, C. L. and Strohaecker, T. R., (2014) "Abrasive wear in Austempered Ductile Irons: A comparison with white cast irons," Wear, vol. 313, no. 1–2, pp. 29–33.

Chaubey S. K. and Gupta K., (2022) "Sustainable Manufacturing of Asymmetric Miniature-Sized Ratchet Wheels by Wire Electrical Discharge Machining," Machines, vol. 10, no. 7.

Conrado E., Gorla C., Davoli P., and Boniardi M., (2017) "A comparison of bending fatigue strength of carburized and nitrided gears for industrial applications," Eng. Fail. Anal., vol. 78, pp. 41–54.

Cular I., Vučković K., Glodež S. and Tonković Z., (2022) "Computational model for bending fatigue prediction of surface hardened spur gears based on the multilayer method," Int. J. Fatigue, vol. 161, p. 106892, Aug.

Davis J. R., (2005) Gear Materials, Properties, and Manufacture. United State of America: ASM International, p. 257-280.

Dommarco R. C. and Salvande J. D., (2003) "Contact fatigue resistance of austempered and partially chilled ductile irons," Wear, vol. 254, no. 3–4, pp. 230–236.

Escobar A., Celentano D., Cruchaga M., and Schulz B., (2015) "On the effect of pouring temperature on spheroidal graphite cast iron solidification," Metals (Basel)., vol. 5, no. 2, pp. 628–647.

Fu Y., Zhuo Y., Zhou X., Wan B., Lv H., and Wang Z., (2020) "Theoretical and experimental study on contact characteristics of spiral bevel gears under quasi-static and large loading conditions," Appl. Sci., vol. 10, no. 15.

Gupta K. and Jain N. K., (2014) "On surface integrity of miniature spur gears manufactured by wire electrical discharge machining," Int. J. Adv. Manuf. Technol., vol. 72, no. 9–12, pp. 1735–1745.

Gupta K. and Jain N. K., (2013) "Manufacturing of High Quality Miniature Gears by Wire Electric Discharge Machining," no. February 2014, pp. 679–696.

Gupta K. R. L. and Jain N. K., (2017) "Advanced Gear Manufacturing and Finishing (Classical and Modern Processes)". London-United Kingdom: Elsevier Ltd., p. 58-129.

Guterres N. D. F. S., Rusnaldy, Widodo A. and Syamsudin A., (2021a) "Investigate Temperature Preheating on the Chill Plate to Identify Surface Characteristic on the Ductile Iron by Sand Casting," Int. J. Eng. Mater. Manuf., vol. 6, no. 3, pp. 141–151.

Guterres N. F. D. S., Rusnaldy and, and Widodo A., (2017a) "Gear distortion analysis due to heat treatment process," in International Conference on Engineering, Science and Nanotechnology 2016 (ICESNANO 2016), vol. 1788.

Guterres N. F. D. S., Rusnaldy, and Widodo A., (2017b) "The Effect of Temperature in Induction Surface Hardening on the Distortion of Gear," in IOP Conference Series: Materials Science and Engineering, vol. 202, no. 1.

Guterres N. F. D. S., Rusnaldy, Widodo A., and Carwita T., (2020b) "The effect of chills thickness to microstructure and surface hardness layer on specimen ductile cast iron," in the 4Th International Conference on Materials and Metallurgical Engineering and

Technology (Icommet) 2020 vol. 2384, no. December, p. 040004.

Hernández -G. C., Marín -G. R. M., Huertas-T. J. L., Efkolidis N., and Kyratsis P., (2016) "WEDM manufacturing method for noncircular gears, using CAD/CAM software," *Stroj. Vestnik/Journal Mech. Eng.*, vol. 62, no. 2, pp. 137–144, doi: 10.5545/sv-jme.2015.2994.

Hurst S., (1996) "METAL CASTING Appropriate technology in the small foundry". London-UK: Intermediate Technology Publications Ltd, p. 123-148.

ISO 6336-1, (2007) "Calculation of load capacity of spur and helical gears: Basic principles, introduction and general influence factors," in International Standard, Second edi., vol. 2007, Switzerland: ISO 2006, p. 109.

ISO 6336-2 (2006) "Calculation of load capacity of spur and helical gears: Calculation of load capacity of spur and helical gear", International Organization for Standardization, vol. 3, p. 16.

ISO 6336-2, (2006) "Calculation of load capacity of spur and helical gears: Calculation of load capacity of spur and helical gear," in International Standard, Second edi., vol. 2006, Switzerland: ISO 2006, p. 33.

ISO 6336-3, (2006) "Calculation of load capacity of spur and helical gears: Calculation of tooth bending strength," in International Organization for Standardization, vol. 3, p. 33.

Beddoes J. and Bibby M. J., *Principles of Metal Manufacturing Processes*. Carleton University, Canada: Elsevier Butterworth-Heinemann p. 284-314.

Jafar K. A. and Behnam A. A., (2011) "Influence of Mold Preheating and Silicon Content on Microstructure and Casting Properties of Ductile Iron in Permanent Mold," *J. Iron Steel Res. Int.*, vol. 18, no. 3, pp. 34–39.

Jamari J., Ammarullah M. I., Afif I. Y., Ismail R., Tauviqirahman M. and Bayuseno A. P., (2021) "Running-in analysis of transmission gear," *Tribol. Ind.*, vol. 43, no. 3, pp. 434–441.

Jaromin M., Dojka R., Jezierski J. and Dojka M., (2019) "Influence of type and shape of the chill on solidification process of steel casting," *Arch. Foundry Eng.*, vol. 19, no. 1, pp. 35–40.

Jenkins L. R., (2005) *ASM Handbook*, Volume 1, Properties and Selection: Irons, Steels, and High Performance Alloys, 10th Editi. United State of America: ASM Handbook, vol. 1, p. 284-314.

Jolivet S., Mezghani S., Mansori E., and Zahouani H., (2013) "Gear noise behavior induced by their topological quality," *Surf. Topogr. Metrol. Prop.*, vol. 2, no. 1, p. 014008, Dec.

Kanthavel K., Arunkumar K., and Vivek S., (2014) "Investigation of chill performance in steel casting process using Response Surface Methodology," *Procedia Eng.*, vol. 97, pp. 329–337.

Kayabasi O. and Erzincanli F., (2007) "Shape optimization of tooth profile of a flexspline for a harmonic drive by finite element modelling," *Mater. Des.*, vol. 28, no. 2, pp. 441–447.

Keyence India PVT. LTD., (2022) "KEYENCE INDIA PVT. LTD", <https://www.keyence.co.in/>, 2022. [Online]. Available: <https://www.keyence.co.in/>. [Accessed: 11-Sep-2022].

Kolivand M. and Kahraman A., (2009) "A load distribution model for hypoid gears using ease-off topography and shell theory," *Mech. Mach. Theory*, vol. 44, no. 10, pp. 1848–1865.

Komori M. et al., (2009) "Evaluation method of lead measurement accuracy of gears using a wedge artefact," *Meas. Sci. Technol.*, vol. 20, no. 2.

Korta J. A. and Mundo D., (2017) "Multi-objective micro-geometry optimization of gear tooth supported by response surface methodology," *Mech. Mach. Theory*, vol. 109, no. June 2016, pp. 278–295.

Kumar M., Ahmad S., and Das M., (2021) "Magneto-rheological-finishing of miniature gear teeth profiles using uniform flow restrictor", vol. 37, no. 4, pp. 467–482.

Kumar P., Sairam C., Hussain M., and Srivastava J. P., (2022) "Investigation on effects of variation of applied load on helical bevel gear made of different materials using simulation technique", *Mater Today Proc.*, Jul. 2022.

Lawson E., (2004) "ANSI/AGMA Accuracy Standards for Gears," *Gear Technol.*, vol. 21, no. 2, pp. 22–26.

Mehr F. F., Reilly C., Cockcroft S., Maijer D., and Mackay R., (2014) "Effect of chill cooling conditions on cooling rate, microstructure and casting/chill interfacial heat transfer coefficient for sand cast A319 alloy," vol. 27, no. 5.

Mott R. L., (2004) *Machine Elements in Mechanical Design*, Fourth Edi. United States of America: Pearson Education, Inc., Upper Saddle River, New Jersey 07458, p. 306-308.

Nisbett B., (2006) *Mechanical Engineering: Shigley's Mechanical Engineering Design*, 8th Editio. United State of America: A Division of The Mc Graw Hill Companies, p. 654-718.

Olawale J. O., Ibitoye, S. A., and Oluwasegun, K. M., (2016) "Processing Techniques and Productions of Ductile Iron: A Review," *Int. J. Sci. Eng. Res.*, vol. 7, no. 9, ISSN 2229-5518, pp. 397–423.

Pavitra H. S. and Anatha P. M. G., (2018) "Study on Microstructure and Mechanical Properties of Al/SiO₂/C hybrid metal matrix composite, with the Influence of Chills," *Mater. Today Proc.*, vol. 5, no. 2, pp. 6053–6058.

Flood S. C., et al. 1998, *ASM Handbook* Vol. 15, "Casting". United State of America: ASM International, University of Oxford, Great Britain. p. 284.

Qian M., Harada S., Kuroshima Y., and Ngayoshi H., (1996) "Surface hardening of ductile cast iron using stainless steel," *Mater. Sci. Eng. A*, vol. 208, no. 1, pp. 88–92.

Radzevich S. P., (2012), "Practical Gear Design and Manufacture", Second Edi. Boca Raton London New York: CRC Press Taylor & Francis Group p. 307-368.

Schneider T., Müller D., Seiler M., Tobie T., Stahl K., and Kästner M., (2022) "Phase-field modeling of fatigue crack growth during tooth flank fracture in case-hardened spur gears," *Int. J. Fatigue*, vol. 163, p. 107091, Oct. 2022.

Sohi M. H., Ebrahimi M., Ghasemi H. M., and Shahripour A., (2012) "Microstructural study of surface melted and chromium surface alloyed ductile iron," *Appl. Surf. Sci.*, vol. 258, no. 19, pp. 7348–7353.

Stöbener D., Freyberg A. V., Fuhrmann M., and Goch G., (2012) "Areal parameters for the characterisation of gear distortions," *Materwiss. Werksttech*, vol. 43, no. 1–2, pp. 120–124.

Sularso and Suga K., (2004) "Dasar Perencanaan dan Pemilihan Elemen Mesin", 11th ed. Jakarta: PT. Pradnya Paramita, Jakarta, p.300.

Von F. A.. and Marc Pillarz A. F., (2020) "Gear shape parameter measurement using a model-based scanning multi-distance measurement approach," *Sensors* (Switzerland), vol. 20, no. 14, pp. 1–16.

Wang J. et al., (2021) "Mathematical simulation and experimental verification of carburizing quenching process based on multi-field coupling," *Coatings*, vol. 11, no. 9.

Wankhede D. M., Narkhede B. E., and Mahajan S. K., (2017) "Investigation of Casting Parameters and External Chills Performance on Mechanical Properties of Aluminum Silicon Alloy (LM6) Castings," no. 7, pp. 4–8.

Wankhede D. M., Narkhede B. E., Mhajan S. K., and Choudhari C. M., (2018) "Influence of pouring temperature and external chills on mechanical properties of aluminum silicon alloy castings," *Mater. Today Proc.*, vol. 5, no. 9, pp. 17627–17635.

Washko S. D. and Aggen G., (1993) *ASM Handbook* Vol. 1 Properties and Selection: Irons Steels and High Performance Alloys, 10 Edition. United State of America: ASM International, p. 2006-2021.

Callister W. D., and Rethwisch Jr. D. G. (2010). *Material Science and Engineering An Introduction* Eighth Ed. John Wiley & Sons, Inc. United States of America. p. 402-405. <https://www.wiley.com/en-us/permissions>.

Yao Y., Chen X., Xing J., Shi L. and Wang Y., (2021) "Tooth Position and Deformation of Flex spline Assembled with Cam in Harmonic Drive Based on Force Analysis," *Chinese J. Mech. Eng.* (English Ed., vol. 34, no. 1.

Zhang Y., Wang G., Pan X., and Li Y., (2022) "Calculating the Load Distribution and Contact Stress of the Disposable Harmonic Drive under Full Load," *Machines*, vol. 10, no. 2.